

EFFECT OF FRICTIONAL HEAT ON THE COEFFICIENT OF FRICTION DURING COMPLETE SLIDE OF AL6061-T6 HERTZIAN CONTACTS**Palani Kumar P**Karpaga Vinayaga College of Engineering and Technology,
Chengalpattu, Chennai, India.palani161984@gmail.com**ABSTRACT:**

In contact tractions, the coefficient of friction (COF) is a key factor and it alters as the contact temperature rises. Therefore, it is crucial to pay attention to how the COF and the increase in contact temperature are related. Since fracture propagation is caused by the existence of the majority load, which can be determined by observing the contact temperature, and crack initiation is caused by the presence of high contact adhesive friction, the transition from full slip circumstances to partial slip conditions is crucial. Using K-type thermocouples adhered close to the contact points along the vertical axis of the cylindrical pad, the contact temperature can be inferred from the measured temperatures. In the current work, the frictional heat flow in the pad is examined during sliding. Finite element analysis (FEA) was used to compare the heat flow in a cylindrical pad with and without insulation. The 1-D heat flow study of the cylindrical pad was carried out using C programming, and the accuracy of the findings was checked against those from the 2-D ANSYS finite element analysis.

Keywords:

Contact temperature, heat flow, full slip fretting, finite element analysis

1. INTRODUCTION

Failure of aerospace structures, offshore structures and nuclear power plant components result in loss of life, disruption of functioning and significant economic losses. Mechanical failure of these structural components is an outcome of material failure due to wear, fatigue and fretting. The riveted joints of aircraft skin structure, gas turbine blades-disk attachment, bolted joints of offshore platforms and steam tubes in nuclear power plants are often subjected to cyclic loads in their normal functioning.

In some of the tightly clamped components which are subjected to cyclic loads, sliding amplitudes of oscillation are very small. This particular phenomenon is known as fretting (Berthier et al., 1989). Fretting effect could initiate cracks at the interface of the sliding bodies. Crack initiation is mainly due to very high stresses near the contact region and propagation of cracks is mainly due to bulk stresses acting on the components. Finally, they lead to failure of the components at levels well below the fatigue limit of the components. This phenomenon is known as fretting fatigue. Following are examples of some practical situations where fretting influences the life of components: gear contacts, bolted and riveted joints, key-way shaft, couplings and blade-dovetail contact regions of turbine engines.

This paper concentrates on frictional heat transfer analysis in cylindrical pad. A detailed steady state heat transfer analysis is performed to study the effect of boundary conditions on the heat flow through cylindrical pad. This study will be used to observe variation of temperature along the cylindrical pad to determine locations of thermocouples to be pasted on the cylindrical pad to observe the frictional heat at the tip of the pad.

2. MATERIALS AND METHODS

Al6061-T6 material was used for the cylindrical pad specimens as shown in Fig. 1. The cylindrical pad is a square rod with cross-section of 6 mm x 6 mm, length 30 mm and with cylindrical edge of 6 mm diameter. Thermal conductivity of Al 6061-T6 was considered as 0.167 W/mm°C for the analysis. The experiments would be

conducted at room temperature with natural convection of the pad. So the convection coefficient of 0.000022 W/mm²°C and the ambient temperature of 28 °C were considered for the analysis from literature (Pulkit Sagar et al., 2016).

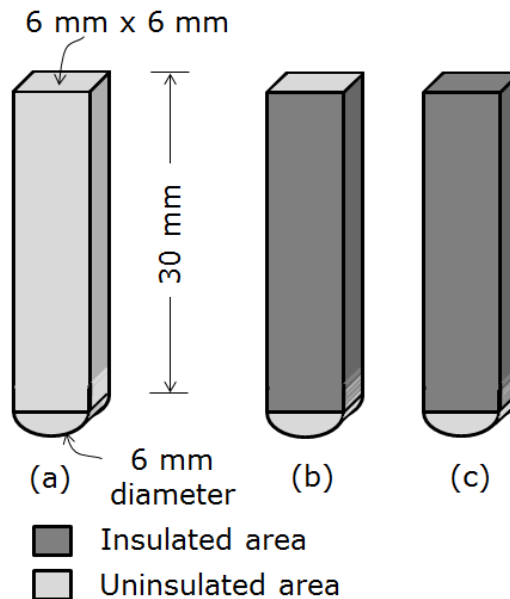


Fig. 1: cylindrical pad (a) without insulation (b) with four side insulation (c) Fully insulation

The one-dimensional conduction steady state analysis was performed by writing code in C-programing language for the fully insulated cylindrical pad. The two-dimensional steady state analysis was performed using ANSYS with different insulation boundary conditions.

3. FINITE ELEMENT ANALYSIS

3.1 One dimensional finite element analysis:

The one-dimensional pure conduction along the pad is considered to develop C program from the basic heat conduction equation (eq. 1) for the 1-D finite element analysis of the insulated pin. The governing equation and boundary conditions of the simple 1D heat flow problem is as follows:

$$\frac{d}{dx} \left(k_x A \frac{dT(x)}{dx} \right) + Q(x)A = 0; x_0 < x < x_L \quad (1)$$

Essential (Dirichlet) boundary conditions:

T = Temperature applied at $x = x_0$ and/or $x = x_L$

Non-essential (Neumann) boundary conditions:

$$\frac{dT}{dx} + \frac{q}{k_x A} = 0, \text{ if specified at bottom end } (x = x_0)$$

$$\frac{dT}{dx} - \frac{q}{k_x A} = 0, \text{ if specified at the top end } (x = x_L)$$

Where k_x = thermal conductivity, A = area of cross section perpendicular to the direction of heat flow, q = heat flux and Q = internal heat generation per unit volume.

The finite element solution is formed by solving eq. (1) using Galerkin's method. The finite element solutions are used to develop C program for 1-D conduction steady state heat transfer. The results obtained from the 1-D C program are given in Fig. 3.

3.2 Two-dimensional finite element analysis:

ANSYS software was used to carry out the finite element analysis in two dimensions. For all cylinder pad combinations, the PLANE55 element was employed. For the conduction and convection analyses of two-dimensional issues, PLANE55 is a four-noded plane element having a single degree of freedom (Temperature) at each node.

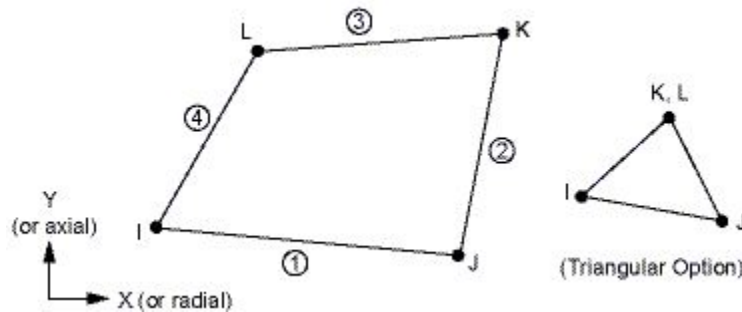


Fig. 2: PLANE55 Element

4. RESULTS AND DISCUSSION

The one-dimensional conductive heat flow analysis was performed on a pad of uniform cross-sectional area and length of 30 mm. The C-programming results of heat flow along the length of the pad are shown in Fig.3. The temperature was linearly decreasing till 20 mm from the pad tip and maintained almost constant temperature till the end of the pad. The variation in temperature is very less in insulated pad.

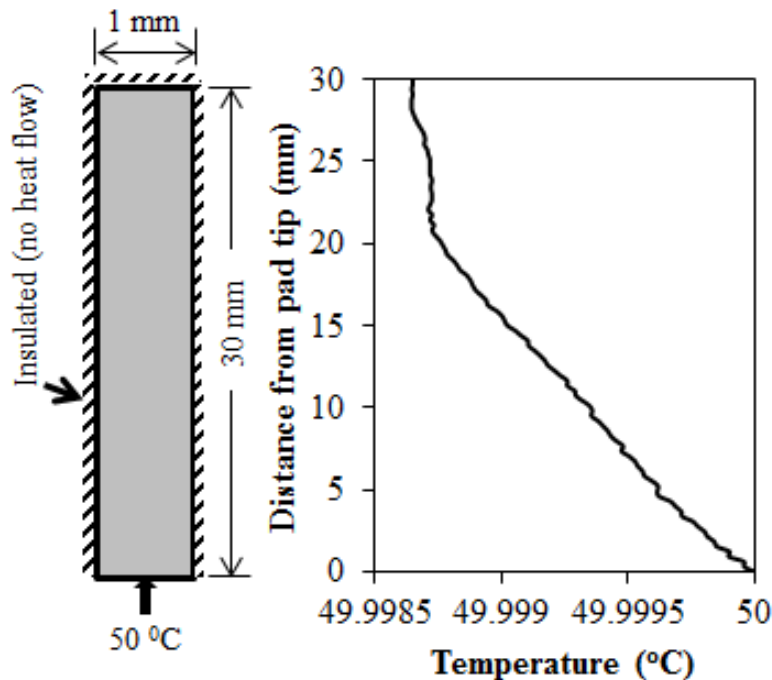


Fig. 3: The heat flow along the length of the pad from 1D-analysis

IJETRM

International Journal of Engineering Technology Research & Management

Published By:

<https://www.ijetrm.com/>

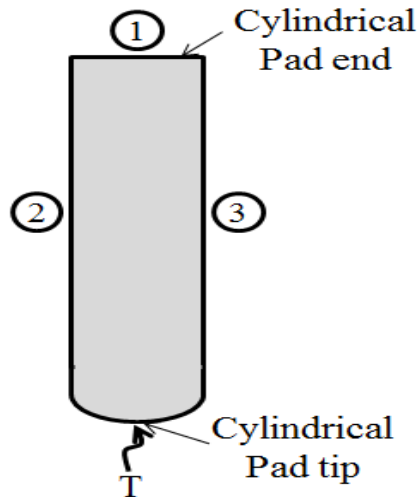


Fig. 4: 2D model of cylindrical pad

Initial studies were focused on effect of insulation on temperature distribution along the cylindrical pad. Fig.4 shows the cylindrical pad with face numbers used for the two-dimensional analysis. The temperature of 50°C was given at pad tip and analysed for the different insulated boundary conditions. A steady state heat transfer analysis was conducted and the results are given in Table 1. The pad without insulation has resulted 1°C variation between the pad tip to pad end temperatures. The fully insulated pad has resulted almost same temperature at the end of the pad compared to the temperature at tip of the pad. The temperature variation along the length of the pad for different insulated boundary conditions is shown from Fig. 5 to Fig. 9.

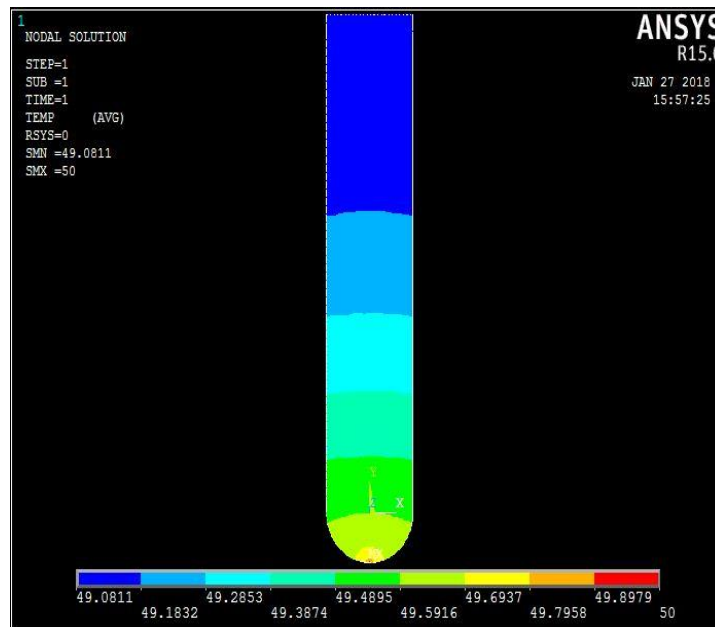


Fig. 5: Temperature distribution in the pin without insulation

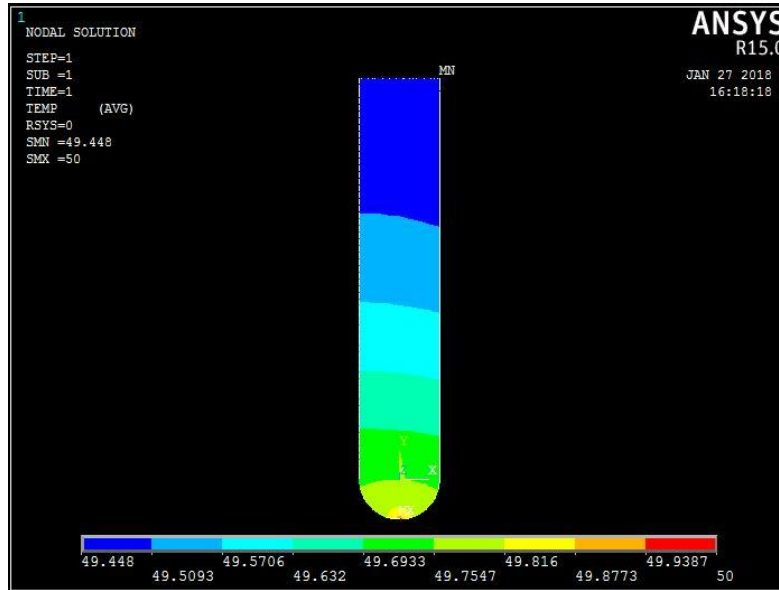


Fig. 6: Temperature distribution in the pin with insulation on side 2

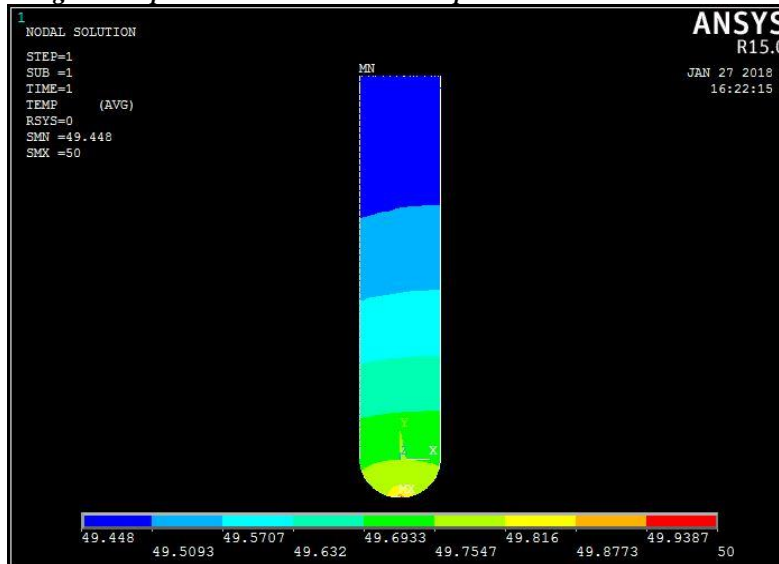


Fig. 7: Temperature distribution in the pin with insulation on side 3

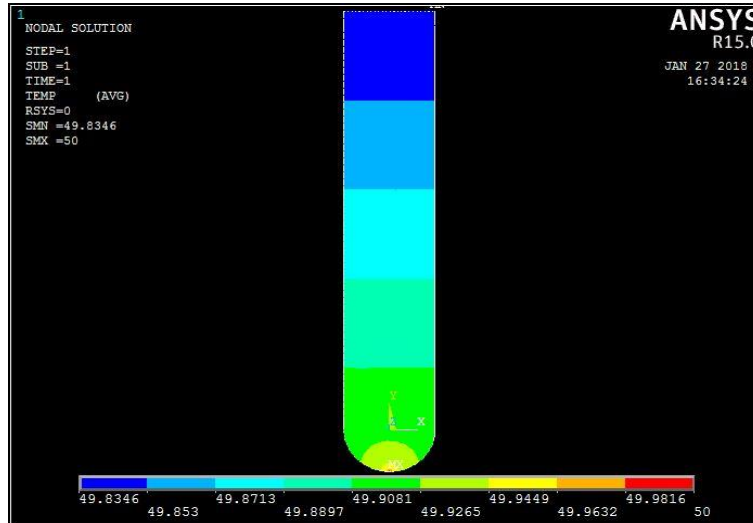


Fig. 8: Temperature distribution in the pin with insulation on side 2 and side 3



Fig. 9: Temperature distribution in the pin with insulation on side 1, side 2 and side 3

Table 1: The temperature at end of the cylindrical pad for different insulated boundary.

Insulated Side	Temperature at pad end (°C)
Without insulation	49.08
1	49.19
2	49.45
3	49.45
1 and 2	49.57
1 and 3	49.57
2 and 3	49.83
1, 2 and 3	49.95

The variation of applied temperature at pad tip to the temperature observed at pad end is less but it depends on the insulation boundary conditions. The second stage of the analysis concentrated on the effect of tip temperature on the temperature at pad end. The applied temperature at pad tip was increased from 30°C to 50°C for pad without insulation and pad with insulation on side 2 and side 3, boundary condition. The variation between the tip temperatures to the pad end temperature is observed with and without insulation on the pad surfaces. It was observed that the variation in temperature is increasing linearly with the increase in temperature applied at pad tip for both insulated and un-insulated pads. The variation in temperature is more when the applied temperature is varying from the ambient temperature in case of un-insulated pad. The pad insulated on side 2 and side 3 gave linear increment in temperature with increase in tip temperature but the variation in the temperature is nearly 1 in 5.5 of the variation in temperature of un-insulated pad. The variation in pad tip to pad end temperature with increase in applied pad tip temperature is given in Fig. 10.

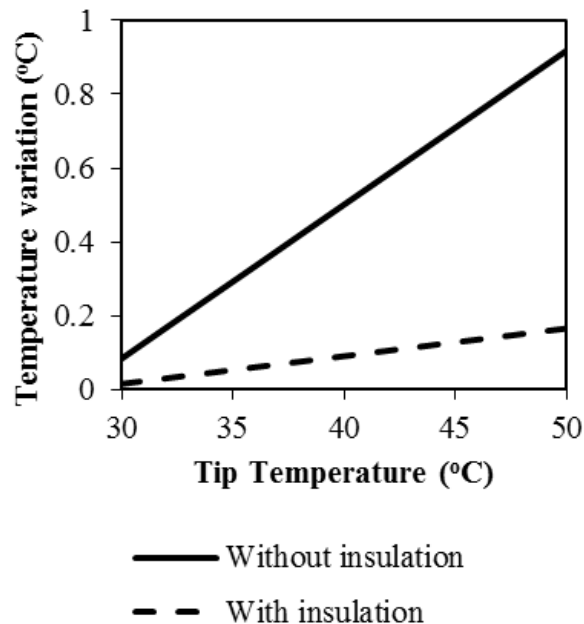


Fig. 10: The temperature variation between pad tip to pad end of un-insulated pad and pad with insulation on side 2 and side 3

Comparison of the 1D heat transfer analysis and 2D heat transfer analysis of fully insulated cylindrical pad gave good agreement of results in both the cases.

5. CONCLUSIONS

The following conclusions have been drawn from the present analysis:

- The temperature at the end side of the pad mainly depends on insulation boundary conditions and temperature at pad tip.
- The temperature variation between pad tip and pad end increases linearly with temperature at pad tip for both insulated and un-insulated pad configurations.
- The temperature variation between pad tip and pad end is always more for un-insulated pad than that for insulated pad.
- The temperature variation between pad tip and pad end of un-insulated pad is 5.5 times than that of the insulated pad.

IJETRM

International Journal of Engineering Technology Research & Management

Published By:

<https://www.ijetrm.com/>

REFERENCES

1. Asghar Bhatti M., (2005), *Fundamental Finite Element Analysis and Applications*, Wiley.
2. Berthier, Y., L. Vincent, and M. Godet (1989). Fretting fatigue and fretting wear, *Tribology international*, vol. 22(4), pp. 235 – 242.
3. Pulkit Sagar, Puneet Teotia, Akash Deep Sahlot, H.C Thakur (2016), Heat transfer analysis and optimization of engine fins of varying geometry, *Materials Today: Proceedings*, Vol. 4 (2017), pp. 8558–8564.
4. Tsirkas S.A., (2018), Numerical simulation of the laser welding process for the prediction of temperature distribution on welded aluminium aircraft components, *Optics and Laser Technology* vol. 100, pp. 45–56
5. Anh Dung Hoang & Joonmo Choung (2021): Effect of heat transfer coefficients on evaluation of temperature distribution in membrane type LNG carriers, *Ships and Offshore Structures*, DOI: 10.1080/17445302.2021.1894029
6. Day, A.J. (2014): *Braking of Road Vehicles*, Elsevier, Amsterdam.
7. Dong, H. Bell, T. (1999): Tribological behaviour of alumina sliding against Ti6Al4V in unlubricated contact, *Wear*, pp. 874–884.
8. *Fundamentals of contact mechanics and friction (2014): Handbook of Friction-Vibration Interactions*, pp.71-152.
9. Giovanni Straffelini (2015): *Friction and Wear: Methodologies for Design and Control*, Switzerland, Springer International Publishing.
10. Giovanni Straffelini, Alberto Molinari, (2011): Mild Sliding Wear of Fe–0.2% C, Ti–6% Al–4% V and Al–7072: A Comparative Study, *Tribology Letters*, Vol. 41, pp. 227-238.
11. Gui, L. Wang, X. Fan, Z. Zhang, F. (2016): A simulation method of thermo-mechanical and tribological coupled analysis in dry sliding systems, *Tribology Int*, Vol. 83, pp. 121–131.
12. H. Murthy and K. Vadivuchezhian, (2016): Estimation of friction distribution in partial-slip contacts from reciprocating full-sliding tests, *Tribology International*, Vol. 108, April 2017, pp. 164-173.
13. Johnson, K. L. (1985): *Contact Mechanics*, Cambridge: Cambridge University Press.
14. J.V. Beck, (1970): Nonlinear estimation applied to the nonlinear inverse heat conduction problem, *Int. J. Heat Mass Transfer*, Vol. 13 (4), pp. 703–716.
15. K. Vadivuchezhian, S. Sundar and H. Murthy, (2011): Effect of variable friction coefficient on contact tractions, *Tribology International*, Vol. 44, pp. 1433 –1442.
16. Kennedy, F.E. Lu, Y. Baker, I. (2015): Contact temperatures and their influence on wear during pin-on-disk tribotesting, *Tribol Int*, Vol. 82, pp. 534–542.
17. K. Imado, A. Miurab, M. Nagatoshia, Y. Kidoc, H. Miyagawab, H. Higaki, (2004): A Study of Contact Temperature Due to Frictional Heating of UHMWPE, *Tribology Letters*, Vol. 16, 265–273.
18. Lim, S. C. Ashby, M. F. Brunton, J. H. (1989): The effects of sliding conditions on the dry friction of metals, *Acta Metallurgica*, Vol. 37, pp. 767-772.
19. M. Hashemzadeh, Y. Garbatov, C. Guedes Soares & A. O'Connor (2021): Friction stir welding induced residual stresses in thick steel plates from experimental and numerical analysis, *Ships and Offshore Structures*, DOI: 10.1080/17445302.2021.1894029
20. Meng, H. C. Ludema, K. C. (2001): *Wear Models and Predictive Equations: Their Form and Content*, *Wear*, pp. 443–457.
21. Maged Elhefnawey et.al, (2020): On dry sliding wear of ECA Ped Al-Mg-Zn alloy: Wear rate and coefficient of friction relationship, *Alexandria Engineering Journal*, pp.1-12.